Surface of room temperature ionic liquid [bmim][PF_6] studied by polarization- and experimental configuration-dependentsum frequency generation vibrational spectroscopy

Ganghua Deng, Yougi Guo, Xia Li, Zhen Zhang, Shilin Liu, Zhou Lu and Yuan Guo

Citation: SCIENCE CHINA Chemistry **58**, 439 (2015); doi: 10.1007/s11426-014-5241-5

View online: http://engine.scichina.com/doi/10.1007/s11426-014-5241-5

View Table of Contents:http://engine.scichina.com/publisher/scp/journal/SCC/58/3

Published by the Science China Press

SCIENCE CHINA Chemistry

SCIENCE CHINA
Chemistry

• ARTICLES •

March 2015 Vol.58 No.3: 439–447
doi: 10.1007/s11426-014-5241-5

Surface of room temperature ionic liquid [bmim][PF_6] studied by polarization- and experimental configuration-dependent sum frequency generation vibrational spectroscopy

Ganghua Deng[1], Youqi Guo[2], Xia Li[3], Zhen Zhang[3], Shilin Liu[1], Zhou Lu[3*] & Yuan Guo[3*]

[1]*Hefei National Laboratory for Physical Sciences at the Microscale, University of Science and Technology of China, Hefei 230026, China*
[2]*Nanjing University of Aeronautics and Astronautics, Nanjing 211106, China*
[3]*Beijing National Laboratory for Molecular Sciences; State Key Laboratory of Molecular Reaction Dynamics; Institute of Chemistry, Chinese Academy of Sciences, Beijing 100190, China*

Received April 23, 2014; accepted May 12, 2014; published online December 10, 2014

Understanding and control of the surface properties such as molecular orientations are of great importance in numerous applications of ionic liquids. However, there remain discrepancies among the previous experimental and theoretical studies on the surface orientation and structures of room temperature ionic liquids (RTIL) systems. In this article, the orientation of 1-butyl-3-methylimidazolium ([bmin]) cation at the air/liquid interface of a characteristic RTIL, 1-butyl-3-methylimidazolium hexafluorophosphate ([bmim][PF_6]), was investigated by the sum frequency generation vibrational spectroscopy (SFG-VS). Detailed polarization and experimental configuration analyses of the SFG-VS spectra showed the possibility of a small spectral splitting in the CH_3 symmetric stretching region, which can be further attributed to the probable existence of multiple orientations for the interfacial [bmim] cations. In addition, the (N)–CH_3 vibrations were absent, ruling out the prediction by several recent molecular dynamics simulations which state that portions of the [bmim] cations orient with a standing-up (N)–CH_3 group at the ionic liquid surface. Hence, new realistic theoretical models have to be developed to reflect the complex nature of the ionic liquid surface.

ionic liquid, sum frequency generation vibrational spectroscopy, interface, orientation

1 Introduction

Room temperature ionic liquids (RTILs) are molten salts characterized by their low melting points (<100 °C), wide liquidus ranges [1], negligible vapor pressures [2], high conductivity [3], large electrochemical windows [4], and good thermal stabilities [5]. Owing to these excellent technical advantages, RTILs have shown great potentials in a variety of applications, including catalysis [6], electrochemistry [7], synthesis [8], separation [9], and green chemistry [10], many of which involve chemical or physical processes on the RTIL surface. As a result, a great number of experimental and theoretical efforts have been made to investigate the surface structure of ionic liquids using various techniques such as surface tension measurements [11], X-ray/neutron reflectivity [12,13], sum frequency generation vibrational spectroscopy (SFG-VS) [14–16] and molecular dynamics (MD) simulations [17–20]. In this study, the polarization and experimental configuration-dependent SFG-VS was employed to explore the orientational structures of the interfacial 1-butyl-3-methylimidazolium hexafluorophosphate ([bmim][PF_6]) on a molecular level.

The [bmim][PF_6] is a typical member in the RTIL family

*Corresponding authors (email: zhoulu@iccas.ac.cn; guoyuan@iccas.ac.cn)

based on the 1-alkyl-3-methyl-imidazolium ([$C_nC_1$im]) cations (Figure 1). Its cationic part [bmim] consists of a positively charged, hydrophilic head (methylimidazolium) and a hydrophobic alkane chain tail, resulting in unique intramolecular polar/nonpolar phase separations in the interfacial layers of ionic liquids [21]. Lately, the orientations and molecular arrangements of the [bmim] and other [$C_nC_1$im] cations at the gas/ionic liquid interface have been intensively investigated due to their crucial roles in determination of the important surface properties, such as surface tension, viscosity, and the capability to accommodate or react with the foreign molecules/ions [11,22–25]. However, inconsistencies are often found among various literature using different types of methods to study the RTIL surfaces [12,14,22,26].

Baldelli's group [14] and Kim's group [15] carried out some of the pioneering SFG-VS studies on the molecular orientations of interfacial [bmim][PF_6] and 1-butyl-3-methylimidazolium tetrafluoroborate ([bmim][BF_4]). Both reported that the butyl chain protrudes into the air. Moreover, Baldelli's group [14] explored the influence of the water vapor pressure on the cation orientations and concluded that at low water pressures ($<10^{-4}$ torr) the imidazolium ring in the [bmim] cation lies nearly parallel to the surface; while at the elevating water pressures, the imidazolium ring adopts a tilting angle of 40°–55° from the surface normal. In contrast, a direct recoil spectroscopy (DRS) measurement yielded completely different results, suggesting that the imidazolium ring is perpendicular to the surface plane with the C(2)–H pointing to the vacuum side, while the butyl chain as well as the 3-methyl group lies close to parallel with the surface for [bmim][PF_6] [22,26]. Of late, both the angle-resolved X-ray photoelectron spectroscopy (AR-XPS) [27] and the high-resolution Rutherford backscattering spectroscopy (HRBS) [28] measurements reported that the butyl chain orients away from the bulk phase into the vacuum, therefore are more consistent with the SFG-VS measurements rather than the DRS experiment. Studies also suggest that ionic liquid surfaces have more inhomogeneous structures along the surface normal: neutron reflectometry (NR) studies on [bmim][BF_4] implied that cationic heads and alkyl tails segregate at the surface to form a lamellar structure which extends to at least two tiers of alkyl groups [13].

Several MD simulations have been carried out to build theoretical models for the [bmim][PF_6] interface. Lynden-Bell *et al.* [18] predicted that the N–N axis in the imidazolium ring adopts a standing-up orientation at the [bmim][PF_6] surface, with the butyl chain pointing into the vacuum and the 3-methyl into the liquid phase. Another MD simulation on [bmim][PF_6] suggested a more complex orientational structure [17], in which two orientations coexist at the [bmim][PF_6] surface: besides the cation orientation similar to what was predicted by Lynden-Bell *et al.*, some imidazolium rings were shown to lie parallel to the surface. Another recent MD simulation on [bmim][PF_6] also proposed that a small portion of the [bmim] cations at the surface can adopt a third orientation with which the 3-methyl group points into the vacuum side and the butyl chain into the liquid phase [20].

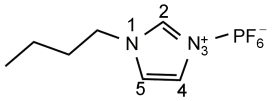

Figure 1 The molecular structure of [bmim][PF_6]. The atoms in the imidazolium ring were numbered for the ease of discussion.

To validate these different theoretical predictions and help understand discrepancies from different experiments, new experimental investigations on the gas/RTIL interface are of utmost significance. In this study, we reexamine the microscopic structures of the air/[bmim][PF_6] interface with the polarization- and experimental configuration-dependent SFG-VS, a surface-selective spectroscopic tool which has recently been proven particularly efficient in identifying orientations of interfacial molecular groups [29,30]. We have compared the SFG-VS spectra obtained under different incident angles of the incoming laser beams. Detailed spectral analyses of the SFG-VS in the CH_3 symmetric stretching region indicated that there might be more than one [bmim] orientation at the RTIL surface. The spectroscopic observations have been compared with the previous MD simulations, which showed that there still remains a gap between the experimental results and theoretical models for the RTIL surfaces.

2 Experimental

2.1 The basic theory of SFG

The details of the SFG-VS theory can be found in several literature [31,32], therefore will only be briefly reviewed here. In an SFG-VS experiment, two laser beams, a visible beam with the frequency of ω_{vis} and the other infrared (IR) beam with the frequency of ω_{IR}, are spatially and temporally overlapped with each other on an interface. By tuning the IR frequency and detecting the sum frequency signal ($\omega_{\text{SF}}=\omega_{\text{vis}}+\omega_{\text{IR}}$), the surface-selective vibrational spectra was obtained with the enhancement of SFG-VS signals given the IR frequency was in resonance with the vibrational transition of the surface species. The sum-frequency (SF) intensity is given by:

$$\begin{aligned} I_{\text{SF}} &\propto (\sec^2\beta_{\text{SF}})\left|\chi^{(2)}_{\text{eff}}\right|^2 \\ &= (\sec^2\beta_{\text{SF}})\left|\chi^{(2)}_{\text{NR}}+\sum_q \frac{A_q}{\omega_{\text{IR}}-\omega_q+i\Gamma_q}\right|^2 \end{aligned} \quad (1)$$

where β_{SF} is the output angle of the sum frequency signal beam against the surface normal; χ_{NR} denotes the non-resonant SFG term; A_q, ω_q and Γ_q represent the sum frequency strength factor tensor, resonant frequency and

damping constant of the qth vibrational mode, respectively; χ_{eff} is the effective second order susceptibility. For a rotationally isotropic liquid interface (C_∞ symmetry), χ_{eff} in the four commonly used polarization combinations can be deduced from the seven nonzero macroscopic susceptibility tensors [31]:

$$\begin{aligned}
\chi^{(2)}_{\text{eff,ssp}} &= L_{yy}(\omega_{\text{SF}})L_{yy}(\omega_{\text{vis}})L_{zz}(\omega_{\text{IR}})\sin\beta_{\text{IR}}\chi^{(2)}_{yyz}\\
\chi^{(2)}_{\text{eff,sps}} &= L_{yy}(\omega_{\text{SF}})L_{zz}(\omega_{\text{vis}})L_{yy}(\omega_{\text{IR}})\sin\beta_{\text{vis}}\chi^{(2)}_{yzy}\\
\chi^{(2)}_{\text{eff,pss}} &= L_{zz}(\omega_{\text{SF}})L_{yy}(\omega_{\text{vis}})L_{yy}(\omega_{\text{IR}})\sin\beta_{\text{SF}}\chi^{(2)}_{zyy}\\
\chi^{(2)}_{\text{eff,ppp}} &= -L_{xx}(\omega_{\text{SF}})L_{xx}(\omega_{\text{vis}})L_{zz}(\omega_{\text{IR}})\cos\beta_{\text{SF}}\times\\
&\quad \cos\beta_{\text{vis}}\sin\beta_{\text{IR}}\chi^{(2)}_{xxz}\\
&\quad -L_{xx}(\omega_{\text{SF}})L_{zz}(\omega_{\text{vis}})L_{xx}(\omega_{\text{IR}})\cos\beta_{\text{SF}}\times\\
&\quad \sin\beta_{\text{vis}}\cos\beta_{\text{IR}}\chi^{(2)}_{xzx}\\
&\quad +L_{zz}(\omega_{\text{SF}})L_{xx}(\omega_{\text{vis}})L_{xx}(\omega_{\text{IR}})\sin\beta_{\text{SF}}\times\\
&\quad \cos\beta_{\text{vis}}\cos\beta_{\text{IR}}\chi^{(2)}_{zxx}\\
&\quad +L_{zz}(\omega_{\text{SF}})L_{zz}(\omega_{\text{vis}})L_{zz}(\omega_{\text{IR}})\sin\beta_{\text{SF}}\times\\
&\quad \sin\beta_{\text{vis}}\sin\beta_{\text{IR}}\chi^{(2)}_{zzz}
\end{aligned} \tag{2}$$

where the polarization index (ssp, sps, pss and ppp) is defined by the polarizations in the order of the SFG, visible and IR beams; ω_{SF}, ω_{vis} and ω_{IR} are the frequencies of the sum frequency signal, incident visible and IR laser beams, respectively; β_{vis} and β_{IR} are the incident angles of the visible and IR beams against the surface normal; xy plane is defined as the plane of the interface in the laboratory coordinates system (x, y, z), and z is the interface normal; L_{ii} (i= x, y, z) is the Fresnel coefficient determined by the refractive indices of the two bulk phase, the effective refractive index of the interface layer (n'), and the incident and reflected angles (β_{vis}, β_{IR} and β_{SF}). The χ_{ijk} tensors are related to the molecular hyperpolarizability tensors β_{ijk} by:

$$\chi^{(2)}_{ijk} = N_{\text{S}}\sum_{i'j'k'}\left\langle R_{ii'}R_{jj'}R_{kk'}\right\rangle\beta^{(2)}_{i'j'k'} \tag{3}$$

Here, N_{S} is the surface density of the molecules, and $\left\langle R_{ii'}R_{jj'}R_{kk'}\right\rangle$ denotes the ensemble average over all of the possible molecular orientations through the Euler rotational transformation matrix R between the laboratory coordinate system (i, j, k) and the molecular coordinate system (i', j', k'). Eq. (3) provides the possibility for using SFG-VS to study the interfacial molecular orientations and their distributions.

2.2 Apparatus

The EKSPLA SFG-VS spectrometer used in the present work has been described in detail previously [33,34]. The 10 Hz and 23 picosecond visible and infrared laser beams were arranged in a co-propagating configuration and were overlapped at the liquid surface of [bmim][PF_6]. The visible wavelength was fixed at 532 nm and the full range of the IR tunability was 1000–4000 cm^{-1}. During the experiment, the laser pulse energy was set at 180 and 200 μJ for the visible and the IR beams, respectively. Four different sets of visible and infrared incident angles (β) were used, which were β_{vis}= 37° & β_{IR}=58° (Config.1), β_{vis}=55° & β_{IR}=41° (Config.2), β_{vis}=63° & β_{IR}=48° (Config.3) and β_{vis}=71° & β_{IR}=48° (Config.4). At each experimental configuration, the SFG spectra were recorded with the combination of both ssp and ppp polarization. The SFG signals were collected in a reflective geometry, guided into a monochromator (Solar TII, MS 3501), and finally recorded by an integrated detection system consisting of a high-gain low-noise photomultiplier (Hamamatsu, PMT-R585) and a dual channel Boxcar averager (Stanford Research Systems). The voltage of R585 was set at 1300 V for the RTIL measurement. During the data acquisition, the IR frequency was scanned with a 2 cm^{-1} increment. The average of all the spectra were achieved by considering two scans each; and 200 laser pulses per point were accumulated for each scan. The SFG-VS spectral resolution in this work was <6 cm^{-1} for the whole 1000–4000 cm^{-1}. Each spectrum was normalized by the SFG spectrum from the Z-cut quartz, following the previously established protocols [34,35]. The measurements were carried out at the controlled room temperature (22.0±0.5 °C) and humidity (40%). The whole experimental setup on the optical table was covered in a plastic housing to reduce the air flow.

2.3 Sample preparation

The RTIL [bmim][PF_6] (>99%) was purchased from Alfa (USA) and used without further purification. The sample was filled in a round Teflon beaker (diameter 5 cm) which was cleaned in advance by first immersing in the Piranha solution for several hours, followed by rinsing with the ultrapure water obtained from the standard Millipore treatment (18.2 MΩ cm).

3 Results and discussion

Figure 2 shows the Z-cut-α-quartz normalized SFG spectra of the air/[bmim][PF_6] interface in the C–H stretching region. Four experimental configurations using different laser incident angles as described in Section 2 were employed. The incident angles of Config.2 (β_{vis}=55° & β_{IR}=41°) and Config.4 (β_{vis}=71° & β_{IR}=48°) were similar to the ones used by Baldelli *et al*. [14,36] and Kim *et al*. [15,37], respectively. As shown in Figure 2, the ppp spectra changed drastically when the incident angles were altered, whereas the ssp spectral line shapes were similar to each other for all the experimental configurations. This happened as the SFG-VS spectra with the ppp polarization are a result of the constructive or destructive interferences of four different

second-order susceptibility (χ_{ijk}) tensors as described in Eq. (2) [31,32]. Since each susceptibility tensor has a coefficient that is a function of the incident angles of incoming laser beams; when the laser incident angles change, the interference among the four ppp susceptibility terms alters accordingly, producing different spectral line shapes [38,39]. On the other hand, only one second-order susceptibility tensor is involved in the ssp spectra. Consequently, laser incident angles only affect the overall spectral intensities for ssp polarizations, and not the spectral line shapes. The different SFG-VS line shapes between ssp and ppp polarization combinations, as well as the dependence of the ppp spectra on different experimental geometries can be quite useful for resolving the structural details, assigning complex SFG-VS spectra, and identifying molecular orientations of the interfacial species [38,39]. The ssp and the ppp spectra from the four experimental configurations (Figure 2) have been analyzed to investigate the possible [bmim] orientations at the air/[bmim][PF_6] interface.

In Figure 2, there are five apparent SFG-VS peaks which have been previously assigned [14,15,36]. In addition, there is a very weak 2913 cm^{-1} feature in the ssp spectra which might be from the CH_2 Fermi resonance. The details of the spectral assignments are summarized in Table 1. The s.s. mode of the CH_3 group directly connected to the imidazolium ring is supposed to be centered either around 2970 cm^{-1} according to the IR and Raman spectra of deuterated

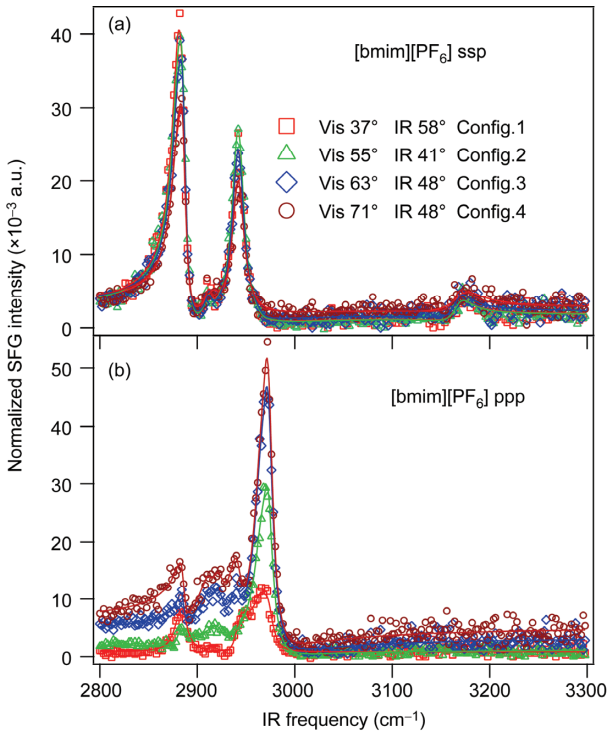

Figure 2 SFG-VS spectra of the air/[bmim][PF_6] interface using two polarization combinations (ssp (a) and ppp (b)) and four different experimental configurations. Config.1: β_{vis}=37°, β_{IR}=58°; Config.2: β_{vis}=55°, β_{IR}=41°; Config.3: β_{vis}=63°, β_{IR}=48°; Config.4: β_{vis}=71°, β_{IR}=48°. The solid lines are the global fitting results using Lorentzian line shapes described by Eq. (1).

Table 1 SFG-VS peak positions and assignments for the air/[bmim] interface

Peak position (cm^{-1})	Assignment
2884	CH_3 s.s.[a)] [14,15,36]
2913	CH_2 Fermi [b)]
2924	CH_2 a.s.[c)] [15]
2945	CH_3 Fermi [14,15,36]
2970	CH_3 a.s. [14,15,36]
3170	H–C(4)–C(5)–H s.s. [14,36]

a) s.s.: symmetric stretch; b) tentative assignment from the current study; c) a.s.: antisymmetric stretch.

[bmim][PF_6] [36] or around 2991 cm^{-1} based on a previous SFG-VS study on the [bmim][PF_6]/quartz interface [40]. Due to the polarization selection rule in SFG-VS, this (N)–CH_3 s.s. mode is expected to appear in the ssp spectra if the methyl group tilts away from the RTIL surface [14,36]. However, neither the current study nor the previous SFG-VS works on the gas/[bmim][PF_6] interface [14,36] showed any noticeable ssp features in the IR frequency regions of ~2970 or ~2991 cm^{-1}, which implies that the (N)–CH_3 group on the 3-methylimidazolium ring probably lies relatively flat at the air/[bmim][PF_6] interface [14,36].

The ppp spectra of the air/[bmim][PF_6] interface changed drastically with the different configurations, especially in the CH_3 s.s. region for the butyl chain in the [bmim] cation. To better illustrate these changes, the expanded portions of the ppp spectra in the 2840–2920 cm^{-1} region were plotted in Figure 3. The corresponding parts of the ssp spectra in the same expanded scale can be found in Figure S1 (Supporting Information online). The discussions in the rest of this paper will be focused on the CH_3 s.s. mode accordingly.

For accurate quantification and interpretation of the data, two different fitting methods were tried, to fit the SFG-VS spectra; an individual fitting procedure in which each spectrum was fitted separately with a single CH_3 s.s. peak, and a global fitting procedure in which all the spectra were fitted simultaneously with two CH_3 s.s. peaks. To be more specific, in the first attempt, each of the ppp spectra was fitted individually with one CH_3 s.s. peak (~2884 cm^{-1}) and the other three apparent ppp peaks of around 2924, 2943 and 2972 cm^{-1}. Similarly, each ssp spectrum was also fitted separately with a single CH_3 s.s. peak (~2884 cm^{-1}) and the other apparent ssp peaks around 2913, 2943 and 3170 cm^{-1}. The fitting parameters obtained for the CH_3 (butyl chain) s.s. mode are listed in Table 2 and those for the other vibrational modes can be found in Table S1 (ssp) and Table S2 (ppp) (Supporting Information online). It could be seen that the individual fitting procedure with a single CH_3 s.s. peak reproduced the SFG-VS spectra effectively from different experimental configurations (Figure 1(a) for ppp and Figure S1(a) for ssp); however, it resulted in noticeable discrepancies for the peak position and width of the CH_3 s.s. peak in the ppp spectra (Table 2).

Table 2 shows that the ssp spectra yield exceedingly similar

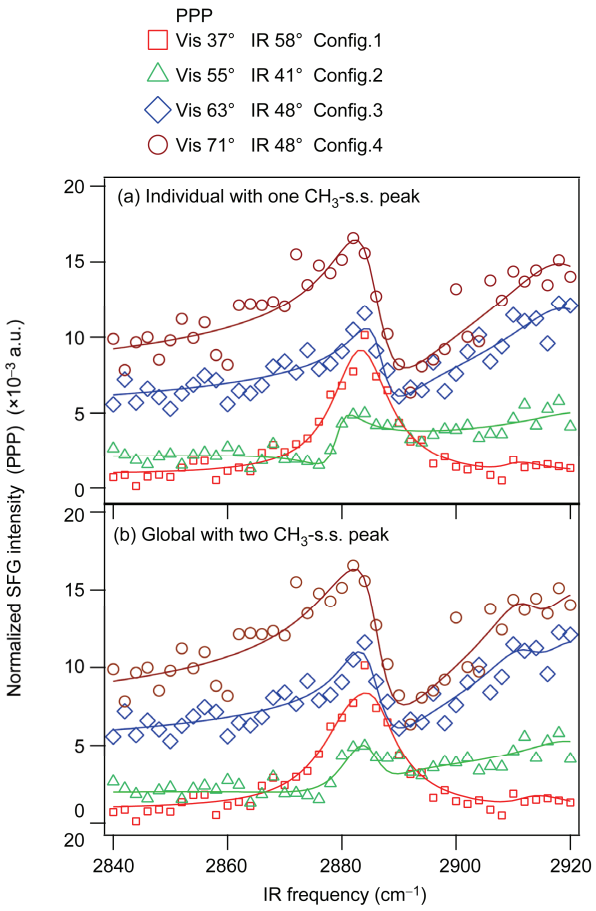

Figure 3 The expanded portion of SFG-VS spectra in the CH_3 (butyl chain) s.s. vibrational region for the air/[bmim][PF_6] interface using the ppp polarization combination and four different experimental configurations. The solid lines represent the fitting results when (a) each ppp spectrum was fitted individually with a single CH_3 s.s. peak and three other apparent ppp peaks (~2924, ~2943 and ~2972 cm^{-1}); (b) all the ppp and ssp spectra were fitted globally with two CH_3 s.s. peaks and five other ssp or ppp peaks (~2913, ~2924, ~2943, ~2972 and ~3170 cm^{-1}).

fitting parameters for different experimental configurations, consistent with the fact that there is no dependence of the ssp spectral line shapes on the laser incident angles as discussed earlier in this section. In the sharp contrast, the fitting parameters of ppp spectra show significant dependence on the experimental configurations. The ppp A_q values change signs when the experimental configurations change from Config.1 to Config.4. And the ppp peak position ω_q jumps from 2879 to 2887 cm^{-1} when the configuration changes from Config.2 to Config.3. Similarly, the peak width (Γ_q) becomes narrower from 6.0 to 2.6 cm^{-1} as the configuration changes from Config.1 to Config.2, and then increases from 3.1 to 4.7 cm^{-1} when the configuration is switched from Config.3 to Config.4.

The dependence of the ω_q and Γ_q values on the laser incident angles was unexpected since the peak position ω_q corresponds to the resonant frequency and the width Γ_q is determined by the vibrational dephasing time. Both ω_q and Γ_q are intrinsic molecular properties of the interfacial species and their chemical surroundings. Therefore neither ω_q nor Γ_q shall change with the experimental configurations. One possible explanation of the observed ω_q and Γ_q variations for the ppp polarization at different experimental configurations is the existence of more than one SFG-VS peak in the butyl CH_3 s.s. vibrational region. Incidentally, the interference between the multiple ppp peaks in this region will depend on the incident angles of laser beams, resulting in the different apparent peak positions and widths.

To further investigate the possible existence of multiple peaks in the CH_3 s.s. region, a second fitting procedure (global fitting) was used, in which all the ssp and ppp spectra in Figure 2(a) and (b) were simultaneously fitted using two CH_3 s.s. peaks with other observed apparent peaks. The expanded portions of the fitting results in the CH_3 (butyl

Table 2 The fitting parameters for the CH_3 (butyl chain) s.s. mode in the ssp and ppp SFG spectra at the air/[bmim][PF_6] interface with the two different fitting methods corresponding to the Figure 3(a) and (c), respectively [a)]

Parameter		Individual with a single CH_3 s.s. peak		Global with two CH_3 s.s. peaks			
				Peak 1		Peak 2	
		ssp	ppp	ssp	ppp	ssp	ppp
ω_q (cm^{-1})	Config.1	2883.4±0.1	2883.3±0.5	2882.2±0.5		2885.7±0.2	
	Config.2	2884.3±0.2	2879.3±0.5				
	Config.3	2884.2±0.1	2886.7±0.6				
	Config.4	2884.5±0.2	2885.6±0.5				
Γ_q (cm^{-1})	Config.1	6.8±0.2	6.0±0.4	7.2±0.2		4.1±0.5	
	Config.2	7.3±0.3	2.6±0.6				
	Config.3	6.4±0.2	3.1±0.9				
	Config.4	6.6±0.2	4.7±0.7				
A_q	Config.1	1.24±0.03	–0.54±0.03	1.05±0.1	–0.54±0.08	0.21±0.1	–0.07±0.06
	Config.2	1.27±0.04	–0.08±0.02	0.88±0.13	–0.24±0.05	0.31±0.11	0.12±0.03
	Config.3	1.11±0.03	0.09±0.02	0.80±0.13	–0.07±0.04	0.33±0.11	0.15±0.03
	Config.4	1.08±0.04	0.23±0.03	0.70±0.11	0.05±0.05	0.30±0.1	0.19±0.04

a) The detailed description of the fitting procedure can be found in the main text. The spectra were fitted with a Lorentzian line shape function (Eq. (1)). The fitting parameters included the resonant vibrational frequency ω_q, the peak width Γ_q, and the spectral amplitudes A_q.

chain) s.s. vibrational region using this global fitting procedure are compared with the experimental spectra in Figure 3(b) for the ppp polarization combination. The ssp fitting results can be found in Figure S1(b). The resultant fitting parameters are listed for the CH_3 s.s. mode and other vibrational modes in Table 2 and Table S3 (Supporting Information online), respectively.

It can be seen that the global fitting with the double CH_3 s.s. peaks can efficiently reproduce the spectral line shapes of the air/[bmim][PF_6] interface for all of the four configurations (Figure 3(b)), and the two CH_3 s.s. vibrations were only 3–4 cm^{-1} apart (Table 2). The obtained spectral amplitudes A_q of the two CH_3 s.s. peaks have the same sign for the ssp spectra irrespective of the experimental configurations used. On the contrary, the phase/sign change of A_q's in the ppp spectra was quite surprising. The A_q's for the two CH_3 s.s. peaks in the ppp spectra using either Config.1 or Config.4 are of the same sign; whereas in Config.2 or Config.3 they are of the opposite signs but have comparable absolute values. The narrowing of the ppp peaks for the butyl CH_3 s.s. mode in Config.2 and Config.3 (Figure 3) could be rationalized as a result of the destructive interference between the two closely spaced SFG-VS peaks which have opposite phases [32]. In fact, this type of the narrowing of the apparent ppp peak widths owing to destructive interference of the closely spaced ppp peaks at certain experimental configurations was not rare. An example is a recently high-resolution broadband SFG-VS study on the air/dimethyl sulfoxide (DMSO) interface [30]. With a spectral resolution of ~0.6 cm^{-1} in that study, the dependence of apparent ppp peak widths on the different laser incident angles was utilized to resolve a ~2.8 cm^{-1} spectral shift between the two CH_3 groups in the same interfacial DMSO molecule.

Although the 6 cm^{-1} resolution used there was insufficient to resolve a spectral splitting of 3–4 cm^{-1}, here are still some other evidence to support the possible small spectral splitting in the CH_3 s.s. region at the air/[bmim][PF_6] interface. As mentioned earlier in this section, when each ppp spectrum was individually fitted with a single CH_3 s.s. peak, the center wavelength can shift as much as 7 cm^{-1} for different laser incident angles (Table 2). This 7 cm^{-1} discrepancy is larger than the 6 cm^{-1} resolution of our SFG-VS spectrometer, thus implying that only one CH_3 s.s. peak is insufficient to explain the SFG-VS spectra of the [bmim]-[PF_6] surface.

If the above statement is correct about the coexistence of multiple butyl CH_3 s.s. peaks for the air/[bmim][PF_6] interface, it would not be possible to use a single peak (ω_q) and width (Γ_q) for the CH_3 s.s. mode to simultaneously fit all the ssp and ppp spectra from different experimental configurations. To verify it, the ssp and ppp spectra from different experimental geometries were globally fitted using a single CH_3 s.s. peak (Figure S2). Five other apparent ssp or ppp peaks (~2913, ~2924, ~2943, ~2972 and ~3170 cm^{-1}) were also included in this global fitting procedure to reproduce the SFG-VS spectra for the other vibrational modes. As we expected, the fitting results significantly deviated away from the experimental SFG-VS line shapes for Config.2 and Config.3 (Figure S2). This failure of the global fitting procedure using only one CH_3 s.s. peak further imply that more than one CH_3 (butyl chain) s.s. peaks may have to be included to simultaneously reproduce all the spectral line shapes obtained with the four different experimental configurations.

The SFG-VS spectra on the gas/RTIL interface have been extensively studied by the Baldelli group [14] and Kim group [15]. However, this new spectroscopic finding of the possible spectral splitting in the CH_3 s.s. region is only made possible by analyzing the ssp and ppp spectra from several different laser incident configurations, showing the potential of the SFG-VS in revealing the complex surface structures of the RTILs. Nevertheless, a careful high-resolution SFG-VS investigation carried out systematically with several different sets of laser incident angles is expected to provide more insight to such a small spectral splitting. We are currently constructing a high resolution broadband SFG-VS spectrometer with the subwavelength spectral resolution in our own laboratory, aiming to fully resolve this type of spectral ambiguity in the near future.

The probable existence of multi CH_3 s.s. peaks at the [bmim][PF_6] surface, especially with the observation of the opposite signs in A_q's for the two tentatively resolved ppp CH_3 s.s. peaks in some experimental configurations, indicates that the [bmim] cation might adopt more than one tilting angle at the RTIL surface [32]. This experimental result is in partial agreement with some recent MD simulations that also predicts the multi-orientations at the RTIL surfaces [17,20,21], however, not all of the orientational angles suggested by these MD simulations can be confirmed by our SFG-VS data.

For example, an MD study on [bmim][PF_6] by Balasubramanian and coworkers [17] suggested the simultaneous presence of two interfacial cation orientations. They proposed that at the outmost layer of the surface the butyl chain orients along the surface normal and points away from the liquid phase, while the imidazolium ring lies flat along the surface plane (Figure 4(a)); in addition, right below the exposed surface there exists a dense region where the N–N axis in the imidazolium ring is aligned along the surface normal (Figure 4(b)). Therefore both the MD simulations and our new SFG-VS data show the evidence of more than one [bmim] orientation at the RTIL surface.

However, the SFG-VS results and the previous MD simulations do not fully agree with each other. Due to the limited spectral resolution in the current study, we are not yet able to quantitatively analyze the orientational angles of the interfacial [bmim] cations. Interestingly, even the qualitative examination of the current SFG-VS data shows some of

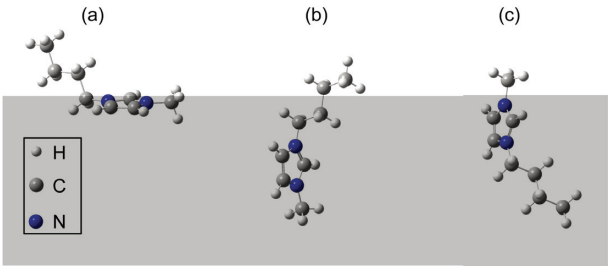

Figure 4 Possible coexisting molecular orientations of air/[bmim][PF_6] interface as predicted by previous MD simulations. (a) The butyl chain points to the vapor phase with the ring lying flat at the surface [14,17,20,36] ; (b) the butyl chain points to the vapor phase with the ring orienting vertically to surface plane [17,18,20]; (c) the (N)–CH_3 group stands up with the ring orienting vertically to surface plane [20].

the orientational angles predicted by the MD simulations might be questionable. According to several MD simulations including that by Balasubramanian and coworker, the [bmim] cations in the dense interfacial region that occupied the majority of the surface populations (~70% according to Lopes and coworkers [2]) were oriented with a vertically-standing (N)–CH_3 group pointing into the liquid phase as shown in Figure 4(b) [17,18,20]. Another possibly coexisting cation orientation proposed by Jorge and coworkers had the (N)–CH_3 group pointing along the surface normal and towards the vapor side (Figure 4(c)). If these two orientations occurred, some of the (N)–CH_3 groups would have tilted along the surface normal and generated a significant amount of the ssp signals either around 2970 cm^{-1} (based on the IR and Raman measurements on the bulk deuterated [bmim][PF_6]) [14,36] or 2991 cm^{-1} (according to a SFG-VS study for the [bmim][PF_6]/quartz interface) [40] for the (N)–CH_3 s.s. mode. But neither this work nor the previous SFG studies [14,36] on the gas/[bmim][PF_6] interface have shown any observable ssp peaks around these frequency regions, thus not supporting the predictions of such molecular orientations.

Furthermore, the previous MD simulations either did not predict the pointing-up (N)–CH_3 group as shown in Figure 4(c) at all [17], or suggested only a small portion (~7%) of the surface [bmim] cations adopted this orientation [20]. Consequently according to these MD simulations, it is not possible for the SFG-VS signals from the two vertically standing (N)–CH_3 with the opposite orientations (Figure 4 (b, c)) to nullify completely and cause the (N)–CH_3 s.s. vibrations invisible.

It also has to be pointed out that in most of the previous MD simulations on the RTIL surface, the upper phase was chosen to be the vacuum or the ideal dry vapor. Some regular contents in the air, such as water molecules, were not considered in the MD simulations. However, our recent SFG-VS study on the low concentrated [bmim][BF_4] aqueous solutions clearly showed that the reorientation process of the interfacial [bmim] cation ring could occur with the changing amount of water in the bulk [41]. For the pure RTIL sample, even [bmim][PF_6], which was traditionally considered as a "hydrophobic" ionic liquid, can easily absorb considerable amount of water molecules when exposed to air [42]. It has been well demonstrated that the existence of only 1 torr of the water pressure in the upper phase can significantly affect the cation ring orientation [14]. The current work was conducted in the air with 40% relative humidity, corresponding to 8 torr partial pressure for water. Thus a theoretical model for the air/[bmim][PF_6] interface should include the influence of the water molecules to be directly compared with the SFG-VS results obtained in the current work. Such a more realistic physical picture of the molecular orientations and arrangements at the air/RTIL surface will be of vital importance since a lot of RTILs applications are not conducted under the vacuum conditions [24,43,44]. However, it is to be noted that the presence of water molecules alone does not fully explain the discrepancies between the SFG-VS measurements and previous MD simulations. A previous SFG-VS experiment on the vacuum/[bmim][PF_6] interface by Baldelli and coworkers [14,36] did not observe any vertically-standing (N)–CH_3 either.

In a summary of the above discussions, the possible spectral splitting in the CH_3 s.s. region of the SFG-VS spectra can be attributed to the existence of two [bmim] orientations at the RTIL surface. So far we can confirm one of the orientations as shown by Figure 4(a) with the butyl CH_3 pointing up to the air and the (N)–CH_3 group lying flat on the surface. But the SFG-VS data do not support the other [bmim] orientations as shown by Figure 4(b, c) with the vertically-standing (N)–CH_3 groups.

4 Conclusions

In this paper, the SFG-VS study on the air/[bmim][PF_6] interface using four different sets of laser incident angles has been presented. The polarization- and experimental configuration-dependent SFG spectra reveal a tentative spectral splitting of ~3–4 cm^{-1} in the CH_3 s.s. region, which implies the possible existence of multiple orientations for the interfacial [bmim] cations. Furthermore, no spectral features of N–CH_3 were observed in the experimental configuration-dependent SFG spectra, proving that the (N)–CH_3 lies flat at the air/[bmim][PF_6] interface. This result does not agree with several recent MD simulation studies which state that some of the interfacial [bmim] cations tilt with the N–CH_3 aligning vertically along the surface normal. It is noteworthy that the quantitative interpretation of these SFG-VS data is still unavailable due to the limitation of the 6 cm^{-1} spectral resolution used in the current work. Further investigation using the high resolution SFG-VS combined with the systematic experimental configuration analysis might facilitate identification of the exact tilting angles and orientational distributions of the [bmim] cations. The systematic SFG-VS analysis employed in this article may also

be useful in studying the complex processes at other RTIL surfaces, such as the IL/aqueous solution interface for the separation protocols [45], and the IL/electrode interface for the electrochemical applications [3,46–48].

Supporting information

The supporting information is available online at chem.scichina.com and link.springer.com/journal/11426. The supporting materials are published as submitted, without typesetting or editing. The responsibility for scientific accuracy and content remains entirely with the authors.

This work was supported by the National Natural Science Foundation of China (21073199, 91027042, 21227802) and the National Basic Research Program of China (2013CB834504).

1 Holbrey JD, Rogers RD. *Ionic Liquids in Synthesis*. 2nd Ed. Weinheim: Wiley-VCH, 2008
2 Esperanca J, Lopes JNC, Tariq M, Santos L, Magee JW, Rebelo LPN. Volatility of aprotic ionic liquids: a review. *J Chem Eng Data*, 2010, 55: 3–12
3 Ohno H. *Electrochemical Aspects of Ionic Liquids*. 2nd Ed. New Jersey: Wiley Hoboken, 2011
4 Suarez PAZ, Selbach VM, Dullius JEL, Einloft S, Piatnicki CMS, Azambuja DS, deSouza RF, Dupont J. Enlarged electrochemical window in dialkyl-imidazolium cation based room-temperature air and water-stable molten salts. *Electrochim Acta*, 1997, 42: 2533–2535
5 Fredlake CP, Crosthwaite JM, Hert DG, Aki S, Brennecke JF. Thermophysical properties of imidazolium-based ionic liquids. *J Chem Eng Data*, 2004, 49: 954–964
6 Sheldon R. Catalytic reactions in ionic liquids. *Chem Commun*, 2001: 2399–2407
7 Liu H, Liu Y, Li J. Ionic liquids in surface electrochemistry. *Phys Chem Chem Phys*, 2010, 12: 1685–1697
8 Cooper ER, Andrews CD, Wheatley PS, Webb PB, Wormald P, Morris RE. Ionic liquids and eutectic mixtures as solvent and template in synthesis of zeolite analogues. *Nature*, 2004, 430: 1012–1016
9 Visser AE, Rogers RD, Room-temperature ionic liquids: new solvents for F-element separations and associated solution chemistry. *J Solid State Chem*, 2003, 171: 109–113
10 Capello C, Fischer U, Hungerbuehler K. What is a green solvent? A Comprehensive framework for the environmental assessment of solvents. *Green Chem*, 2007, 9: 927–934
11 Law G, Watson PR. Surface tension measurements of *N*-alkylimidazolium ionic liquids. *Langmuir*, 2001, 17: 6138–6141
12 Solutskin E, Ocko BM, Taman L, Kuzmenko I, Gog T, Deutsch M. Surface, layering in ionic liquids: an X-ray reflectivity study. *J Am Chem Soc*, 2005, 127: 7796–7804
13 Bowers J, Vergara-Gutierrez MC, Webster JRP. Surface ordering of amphiphilic ionic liquids. *Langmuir*, 2004, 20: 309–312
14 Baldelli S. Influence of water on the orientation of cations at the surface of a room-temperature ionic liquid: a sum frequency generation vibrational spectroscopic study. *J Phys Chem B*, 2003, 107: 6148–6152
15 Iimori T, Iwahashi T, Ishii H, Seki K, Ouchi Y, Ozawa R, Hamaguchi H, Kim D. Orientational ordering of alkyl chain at the air/liquid interface of ionic liquids studied by sum frequency vibrational spectroscopy. *Chem Phys Lett*, 2004, 389: 321–326
16 Santos CS, Rivera-Rubero S, Dibrov S, Baldelli S. Ions at the surface of a room-temperature ionic liquid. *J Phys Chem C*, 2007, 111: 7682–7691
17 Bhargava BL, Balasubramanian S. Lay layering at an ionic liquid-vapor interface: a molecular dynamics simulation study of [bmim][PF_6]. *J Am Chem Soc*, 2006, 128: 10073–10078
18 Lynden-Bell RM, Del Popolo M. Simulation of the surface structure of butylmethylimidazolium ionic liquids. *Phys Chem Chem Phys*, 2006, 8: 949–954
19 Yockel S, Schatz GC. Modeling O(^{3}P) and Ar scattering from the ionic liquid [emim][NO_3] at 5 eV with hybrid QM/MM molecular dynamics. *J Phys Chem B*, 2010, 114: 14241–14248
20 Hantal G, Cordeiro M, Jorge M. What does an ionic liquid surface really look like? Unprecedented details from molecular simulations. *Phys Chem Chem Phys*, 2011, 13: 21230–21232
21 Yan TY, Li S, Jiang W, Gao XP, Xiang B, Voth GA. Structure of the liquid-vacuum interface of room-temperature ionic liquids: a molecular dynamics study. *J Phys Chem B*, 2006, 110: 1800–1806
22 Law G, Watson PR. Surface orientation in ionic liquids. *Chem Phys Lett*, 2001, 345: 1–4
23 Froba AP, Wasserscheid P, Gerhard D, Kremer H, Leipertz A, Revealing the influence of the strength of coulomb interactions on the viscosity and interfacial tension of ionic liquid cosolvent mixtures. *J Phys Chem B*, 2007, 111: 12817–12822
24 Scovazzo P, Kieft J, Finan DA, Koval C, DuBois D, Noble R. Gas separations using non-hexafluorophosphate [PF_6]$^-$ anion supported ionic liquid membranes. *J Membrane Sci*, 2004, 238: 57–63
25 Roscioli JR, Nesbitt DJ. State-resolved scattering at room-temperature ionic liquid-vacuum interfaces: anion dependence and the role of dynamic versus equilibrium effects. *J Phys Chem Lett*, 2010, 1: 674–678
26 Law G, Watson PR, Carmichael AJ, Seddon KR, Seddon B. Molecular composition and orientation at the surface of room-temperature ionic liquids: effect of molecular structure. *Phys Chem Chem Phys*, 2001, 3: 2879–2885
27 Lockett V, Sedev R, Bassell C, Ralston J. Angle-resolved X-ray photoelectron spectroscopy of the surface of imidazolium ionic liquids. *Phys Chem Chem Phys*, 2008, 10: 1330–1335
28 Ohno A, Hashimoto H, Nakajima K, Suzuki M, Kimura K. Observation of surface structure of 1-butyl-3-methylimidazolium hexafluorophosphate using high-resolution rutherford backscattering spectroscopy. *J Chem Phys*, 2009, 130: 204705
29 Zhang Z, Guo Y, Lu Z, Velarde L, Wang HF. Resolving two closely overlapping –CN vibrations and structure in the langmuir mono layer of the long-chain nonadecanenitrile by polarization sum frequency generation vibrational spectroscopy. *J Phys Chem C*, 2012, 116: 2976–2987
30 Velarde L, Zhang XY, Lu Z, Joly AG, Wang ZM, Wang HF. Communication: spectroscopic phase and lineshapes in high-resolution broadband sum frequency vibrational spectroscopy: resolving interfacial inhomogeneities of "identical" molecular groups. *J Chem Phys*, 2011, 135: 241102
31 Zhuang X, Miranda PB, Kim D, Shen YR. Mapping molecular orientation and conformation at interfaces by surface nonlinear optics. *Phys Rev B*, 1999, 59: 12632–12640
32 Wang HF, Gan W, Lu R, Rao Y, Wu BH. Quantitative spectral and orientational analysis in surface sum frequency generation vibrational spectroscopy (SFG-VS). *Int Rev Phys Chem*, 2005, 24: 191–256
33 Lu R, Gan W, Wu BH, Chen H, Wang HF. Vibrational polarization spectroscopy of CH stretching modes of the methylene group at the vapor/liquid interfaces with sum frequency generation. *J Phys Chem B*, 2004, 108: 7297–7306
34 Gan W, Wu D, Zhang Z, Feng RR, Wang HF. Polarization and experimental configuration analyses of sum frequency generation vibrational spectra, structure, and orientational motion of the air/water interface. *J Chem Phys*, 2006, 124: 114705
35 Wei X, Hong SC, Zhuang XW, Goto T, Shen YR. Nonlinear optical studies of liquid crystal alignment on a rubbed polyvinyl alcohol surface. *Phys Rev E*, 2000, 62: 5160–5172
36 Rivera-Rubero S, Baldelli S. Surface characterization of 1-butyl-3-methylimidazollum Br^-, I^-, PF_6^-, BF_4^-, $(CF_3SO_2)_2N^-$, SCN^-, $CH_3SO_3^-$, $CH_3SO_4^-$, and $(CN)_2N^-$ ionic liquids by sum frequency generation. *J Phys Chem B*, 2006, 110: 4756–4765
37 Iwahashi T, Sakai Y, Kanai K, Kim D, Ouchi Y. Alkyl-chain divid-

ing layer at an alcohol/ionic liquid buried interface studied by sum-frequency generation vibrational spectroscopy. *Phys Chem Chem Phys*, 2010, 12: 12943–12946
38 Gan W, Wu BH, Zhang Z, Guo Y, Wang HF. Vibrational spectra and molecular orientation with experimental configuration analysis in surface sum frequency generation (SFG). *J Phys Chem C*, 2007, 111: 8716–8725
39 Gan W, Zhang Z, Feng RR, Wang HF. Spectral interference and molecular conformation at liquid interface with sum frequency generation vibrational spectroscopy (SFG-VS). *J Phys Chem C*, 2007, 111: 8726–8738
40 Rollins JB, Fitchett BD, Conboy JC. Structure and orientation of the imidazolium cation at the room-temperature ionic liquid/sio$_2$ interface measured by sum-frequency vibrational spectroscopy. *J Phys Chem B*, 2007, 111: 4990–4999
41 Deng GH, Li X, Guo YQ, Liu SL, Lu Z, Guo Y. Orientation and structure of ionic liquid cation at air/bmirn BF4 aqueous solution interface. *Chin J Chem Phys*, 2013, 26: 569–575
42 Cammarata L, Kazarian SG, Salter PA, Welton T. Molecular states of water in room temperature ionic liquids. *Phys Chem Chem Phys*, 2001, 3: 5192–5200
43 Plechkova NV, Seddon KR. Applications of ionic liquids in the chemical industry. *Chem Soc Rev*, 2008, 37: 123–150
44 Zhou F, Liang Y, Liu W. Ionic liquid lubricants: designed chemistry for engineering applications. *Chem Soc Rev*, 2009, 38: 2590–2599
45 Han X, Armstrong DW. Ionic liquids in separations. *Acc Chem Res*, 2007, 40: 1079–1086
46 Galinski M, Lewandowski A, Stepniak I. Ionic liquids as electrolytes. *Electrochim Acta*, 2006, 51: 5567–5580
47 Sakaebe H, Matsumoto H. *N*-methyl-*N*-propylpiperidinium bis(trifluoromethanesulfonyl) imide (PP 13-TFSI): novel electrolyte base for Li battery. *Electrochem Commun*, 2003, 5: 594–598
48 Baldelli S. Surface structure at the ionic liquid-electrified metal interface. *Acc Chem Res*, 2008, 41: 421–431